MICROCOPY RESOLUTION TEST CHART
NATIONAL BUREAU

ERL-0072-TR

AR-001-655

LEVEL II

AUSTRALIA

DEPARTMENT OF DEFENCE

DEFENCE SCIENCE AND TECHNOLOGY ORGANISATION
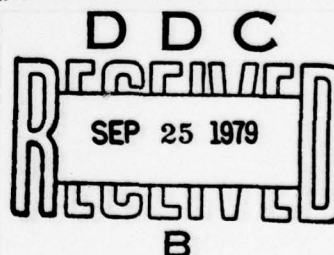
ELECTRONICS RESEARCH LABORATORY

DEFENCE RESEARCH CENTRE SALISBURY
SOUTH AUSTRALIA

TECHNICAL REPORT

ERL-0072-TR

THE INFLUENCE OF WATER TURBIDITY ON THE PERFORMANCE
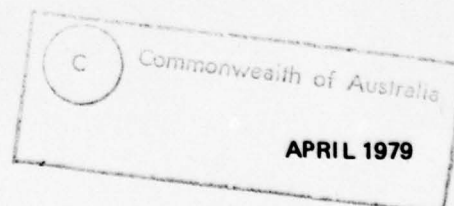# OF A LASER AIRBORNE DEPTH SOUNDER

D.M. PHILLIPS

DDC

RECEIVED

SEP 25 1979

B

DEFENCE SCIENCE AND TECHNOLOGY ORGANISATION

Approved for Public Release.

C Commonwealth of Australia

COPY No. 27

APRIL 1979

UNCLASSIFIED

DEPARTMENT OF DEFENCE   AR-001-655

DEFENCE SCIENCE AND TECHNOLOGY ORGANISATION

ELECTRONICS RESEARCH LABORATORY

(14) ERL-0072-TR   (11) Apr 79

(9) TECHNICAL REPORT

ERL-0072-TR

(6) THE INFLUENCE OF WATER TURBIDITY ON THE PERFORMANCE
OF A LASER AIRBORNE DEPTH SOUNDER

(10)   D.M. Phillips

(12) 29p.

S U M M A R Y

During flight trials of a laser airborne depth sounder
(WRELADS), measurements were made of the optical attenuation
coefficient of coastal waters in both South Australia and
Queensland. Measurements of the attenuation coefficient at
wavelengths from 400 nm to 600 nm are reported for a range of
different water types, and the suitability for depth sounding
of the laser wavelength 532 nm is confirmed. Variations
of the attenuation coefficient at 530 nm over two vertical
sections of sea water are reported and factors influencing the
turbidity are suggested. Return signals recorded by the depth
sounder are compared with measured attenuation coefficients of
the water. It is shown that the maximum measurable water
depth varies from below 4 to above 10 attenuation lengths,
depending on the turbidity of the water.

Approved for Public Release.

UNCLASSIFIED

410 863

DOCUMENT CONTROL DATA SHEET

Security classification of this page | **UNCLASSIFIED**

1	DOCUMENT NUMBERS		2	SECURITY CLASSIFICATION	

1 DOCUMENT NUMBERS

AR Number:	AR-001-655
Report Number:	ERL-0072-TR ✓
Other Numbers:	

2 SECURITY CLASSIFICATION

a. Complete Document:	UNCLASSIFIED
b. Title in Isolation:	UNCLASSIFIED
c. Summary in Isolation:	UNCLASSIFIED

3 TITLE

THE INFLUENCE OF WATER TURBIDITY ON THE PERFORMANCE OF A LASER AIRBORNE DEPTH SOUNDER

4 PERSONAL AUTHOR(S):

D.M. Phillips

5 DOCUMENT DATE:

April 1979

6

6.1	TOTAL NUMBER OF PAGES	28
6.2	NUMBER OF REFERENCES:	12

7 7.1 CORPORATE AUTHOR(S):

Electronics Research Laboratory ✓

7.2 DOCUMENT SERIES AND NUMBER
Electronics Research Laboratory
0072-TR

8 REFERENCE NUMBERS

a. Task:	NAV 77/020
b. Sponsoring Agency:	NST 1102

9 COST CODE:

313413

10 IMPRINT (Publishing organisation)

Defence Research Centre Salisbury

11 COMPUTER PROGRAM(S)
(Title(s) and language(s))

12 RELEASE LIMITATIONS (of the document):

Approved for Public Release.

12.0	OVERSEAS	NO	P.R.	1	A		B		C		D		E	

Security classification of this page: | UNCLASSIFIED

13 | ANNOUNCEMENT LIMITATIONS (of the information on these pages):

No limitation.

14 | DESCRIPTORS:

a. EJC Thesaurus
Terms

Lasers
Laser beams
Tests
Flight tests
Depth sounding
Optical properties

Airborne equipment
Oceans
Sea water
Turbidity
Opacity

b. Non-Thesaurus
Terms

15 | COSATI CODES:

2005
1701

16 | LIBRARY LOCATION CODES (for libraries listed in the distribution):

17 | SUMMARY OR ABSTRACT:
(if this is security classified, the announcement of this report will be similarly classified)

During flight trials of a laser airborne depth sounder (WRELADS), measurements were made of the optical attenuation coefficient of coastal waters in both South Australia and Queensland. Measurements of the attenuation coefficient at wavelengths from 400 to 600 nm are reported for a range of different water types, and the suitability for depth sounding of the laser wavelength 532 nm is confirmed. Variations of the attenuation coefficient at 530 nm over two vertical sections of sea water are reported and factors influencing the turbidity are suggested. Return signals recorded by the depth sounder are compared with measured attenuation coefficients of the water. It is shown that the maximum measurable water depth varies from below 4 to above 10 attenuation lengths, depending on the turbidity of the water.

ACCESSION for
NTIS   White Section
DDC   Buff Section
UNANNOUNCED
JUSTIFICATION

BY
DISTRIBUTION/AVAILABILITY CODES
Dist.   AVAIL. and/or SPECIAL

A

TABLE OF CONTENTS

LIST OF FIGURES

1. INTRODUCTION

A laser airborne depth sounder (WRELADS) is being developed at the Defence Research Centre Salisbury, to assist the Royal Australian Navy in its task of charting Australian coastal waters. The operation of the system and some preliminary results obtained by it are described by Clegg and Penny(ref.1). The results of feasibility trials in 1975 are described by Abbot and Penny(ref.2) and a detailed report of the first stage of the development program has been written by Abbot et al(ref.3).

Because the depth sounder relies for its operation on the penetration of a laser beam through the water, the performance of the system is limited by the turbidity of the water. It is important, therefore, to know the relationship between the maximum depth that can be measured by the system and the turbidity of the water through which the laser beam must pass.

A quantitative measure of turbidity is the attenuation coefficient, which describes the rate of attenuation of a beam (usually per metre) due to both absorption and scattering. The dependence of the attenuation coefficient on wavelength is shown in figure 1 for several types of sea water. The shaded region represents the range of measured values of the beam attenuation coefficient of pure water, judged by Smith and Tyler(ref.4) to have relatively higher precision and accuracy. Their graph of selected data is also reproduced by Tyler(ref.5). The other curves are derived from measurements by Clarke and James(ref.6) of the attenuance of unfiltered samples of sea water from a variety of locations. The wavelength of 532 n mile from the frequency doubled Nd:YAG laser would seem to be suitable for good penetration in a variety of water types. One of the reasons for the experiments described in this report was to evaluate the suitability of this laser for depth sounding in Australian coastal waters.

The turbidity of Australian coastal waters is not well known. Koerber(ref.7) reports one measurement of the spectral signature of the attenuation coefficient in Gulf St Vincent, SA. Watts(ref.8) has summarized Secchi depth data obtained by the Australian and US Navies. However, the Secchi data are of limited usefulness because the measured values depend on the illumination conditions, they are not spectrally resolved, and it is not clear whether the measurements are of coastal or oceanic water. A second reason for the experiments described below was to measure attenuation coefficients in Australian coastal waters, particularly at wavelengths of about 530 nm, and to understand the marine processes that influence turbidity.

While the water attenuation coefficient was being determined from a boat, the WRELADS system was operated from an aircraft flying overhead. Laser signal returns were recorded showing backscatter of the beam as it penetrated the water and its reflection from the bottom. The third reason for these experiments was to establish an empirical relationship between the maximum measurable water depth and the attenuation coefficient of the water through which the beam passed.

2. WATER TRANSMISSOMETER

The values of the beam attenuation coefficient of water presented in this report were deduced from measurements of beam transmittance. The instrument used to obtain the measurements is described by Woodcock(ref.9). It is a cylindrically limited system of the type described by Austin and Petzold(ref.10). The transmittance of the instrument is given by

$$T = F/F_o = \exp(-cl) , \qquad (1)$$

where F_o and F are the values of the radiant flux in the beam before and after

it has travelled through the water column length ℓ. Since attenuation of the beam is due to both absorption and scattering, the attenuation coefficient is given by

$$c = a + b , \qquad (2)$$

where a is the absorption coefficient and b is the scattering coefficient.

The accuracy of the instrument is limited by the amount of forward scattered light reaching the detector. Thoeretically the beam transmittance should contain no contribution from scattering but in practice small-angle forward scattering does reach the detector. The measured transmittance is then higher than the theoretical value, and the attenuation coefficient determined from the measured transmittance is less than the true value.

The magnitudes of these errors have been estimated by Austin and Petzold(ref.10). In the present instrument the maximum acceptance angle is about 2 degree, although the average acceptance angle is considerably less than that. Nevertheless, the experimentally determined values of attenuation coefficient could underestimate the true values by as much as 20% when the water is relatively turbid. However, an error of this magnitude is still small compared with the uncertainty in the attenuation coefficient of pure water over much of the spectrum, shown in figure 1.

The instrument was calibrated using the air path method described by Austin and Petzold(ref.10). Taking into account the reflection losses at the air glass interfaces, the transmittance in air should be 85%. The gain of the instrument was adjusted until it read the correct value during the calibration. Care was taken in the design to ensure that the cylindrically limited beam passed through the optical system without obstruction in both the air and water cases.

3. MEASUREMENTS IN GULF ST VINCENT

The beam attenuation coefficient of the water along a line of buoys in Gulf St Vincent was determined from transmittance measurements obtained with the instrument described in the previous section. The buoys were accurately placed, by the Division of National Mapping, at 500 m intervals along a line emanating from a point on the coastline 7.5 km by road north of Stansbury on a magnetic bearing of 119 degree, as shown in figure 2. Clusters of four or six buoys in different colours were used to facilitate unique identification of the position. The 35 clusters of such buoys stretched a total distance of 17.5 km from the shore.

The line of buoys runs close to the 6 m water depth contour for much of its length. Towards the end of the line, the depth drops rapidly to about 30 m. About 5 km from the shore, the line runs close to the end of South Spit, a sand spit extending in a north-easterly direction from Stansbury.

The first set of measurements was obtained on 23 November 1976. The water transmittance was measured at 1 m intervals in depth, from the surface down to 10 m and at 2 m intervals beyond that in deep water. All measurements were made with a spectral filter at 530 nm and they were obtained at most buoy positions. These data were used to plot the contours of attenuation coefficient shown in figure 3. The figure presents the measured distribution of the beam attenuation coefficient over a vertical section of the water along the line of buoys. Above the graph are photographs of the bottom at the locations shown, taken on the same day.

In the shallow waters covering the shelf there is clear evidence of strong vertical mixing probably due to wave motion. The deeper water appears to be layered, possibly due to a stable temperature gradient in the warm November weather. The most turbid patch of water detected at about 3 km from the shore

was close to the sand spit, where the bottom consisted of a very fine sand.
The clearest water detected was over very coarse sand on the edge of the
shelf.

Another set of measurements was made about a month later on 17 December
1976. The resulting contours of equal attenuation coefficient are presented
in figure 4. The turbid patch of water close to shore and associated with the
sand spit is seen again and so is the clear patch of water above the edge of
the shelf. Strong vertical mixing is again evident above the shelf. In the
deeper water the horizontal layers evident in figure 3 are absent, although
there is a hint that layering may occur at a greater distance from the shore.
One notable feature of figure 4 is the rapid change in water turbidity at the
edge of the shelf. This suggests a change in the water body on opposite sides
of this interface.

While the water attenuation coefficient measurements were being made from a
boat, the WRELADS system was flown overhead in an aircraft and measurements of
the green return signal were recorded. The oscillograms are reproduced at the
top of figure 4. Oscillograms (a) to (e) were all recorded with the same EHT
voltage on the photomultiplier (1100 V) and hence their amplitudes are
directly comparable. It can be seen that the first pulse (from the water
surface) is variable in amplitude, due to variations in the reflecting facets
of the water surface. The amplitudes of the bottom returns, however, are
governed primarily by the turbidity of the water. Oscillogram (b) which was
recorded about 1.5 km from the shore, where the most turbid water was
observed, had the smallest bottom return. At greater distances from the
shore, bottom returns in oscillograms (c), (d) and (e) steadily increase in
amplitude as the water clarity improves. Oscillograms (f) and (g) were
recorded in similar water with the same EHT voltage on the photomultiplier but
the bottom return in the latter is reduced in amplitude due to the increased
depth of water. Oscillograms (h) and (i) which were recorded with the same
photomultiplier voltage, show a stronger backscatter envelope in the latter
case due to the more turbid water at the surface. In all cases except (i),
the depths measured from the boat agree well with those measured by the
WRELADS system. The discrepancy in the last case is probably due to the plane
flying some distance north of the line of buoys where the shelf extends
further east.

A further set of results obtained on 10 June 1977 is presented in figure 5.
The turbid patch of water close to shore, the clear water at the edge of the
shelf and the strong vertical mixing in the shallow water above the shelf are
again evident. The oscillograms are again correlated with the water turbidity
measurements. The double pulse in many of the surface and bottom returns is
probably due to the laser being incorrectly adjusted and transmitting a double
pulse. Traces (a) and (b), which were recorded with a photomultiplier voltage
of 1200 V, reflect the increased turbidity of the water in the latter case.
The remaining oscillograms (c) and (i) were all recorded with the
photomultiplier voltage of 1250 V and are therefore directly comparable. It
can be seen that the amplitude of the bottom return remains approximately
constant in traces (c), (d) and (e) even though the water depth increases,
because the water clarity also improves. This improvement is so marked in
oscillogram (f) that, even with a substantial increase in depth, the bottom
return saturates the photomultiplier. Traces (g), (h) and (i) show the bottom
return gradually becoming weaker as the depth increases. Trace (i) is an
example of an extinction depth, that is the greatest depth measurable under
those conditions.

4. FACTORS INFLUENCING TURBIDITY

The main factors influencing water turbidity are given by Williams(ref.11)
as:

    1. the nature of the land which borders on the area,

2. the currents in the area,

3. the amount of precipitation in the area,

4. the amount of wind mixing,

5. the type of bottom, and

6. the proximity of civilization.

The measured attenuation coefficients provide some indication of the relative significance of these factors in Gulf St Vincent.

Although drainage from the farmland in the vicinity of Stansbury could increase the turbidity of the coastal water, it is probably not the dominant factor.   With an annual rainfall of only about 400 mm and no rivers, very little runoff would be expected.   Indeed the most turbid water was encountered on 23 November, when no rain had fallen in the area for a week, whereas the greatest rainfall associated with the experiments was 6 mm on the day prior to the second trip.   It is assumed, therefore, that drainage from the land makes a negligible contribution to turbidity in Gulf St Vincent near Stansbury.

The proximity of civilization at Stansbury could increase the turbidity in Oyster Bay which lies between South Spit and the mainland.   The end of the spit lies approximately 5 km from the shore along the line of buoys.   The most turbid region on each of the three trips was located between 1 and 4 km from the shore,   that is at the entrance to Oyster Bay.   Although Stansbury's population (about 400) is small, it could produce some pollution but another possible explanation for the observed turbidity is considered below.

Wind-driven waves stirring up sediment from the bottom appear to be the most significant factor influencing turbidity in shallow water.   Figures 3, 4 and 5 all show nearly vertical contours of equal attenuation coefficient in the shallow water over the shelf.   This is evidence of strong vertical mixing. On all trips, the general features of the water turbidity over the shelf are related to the nature of the bottom determined on the first trip.   The photographs shown in figure 3 provides some indication of the nature of the bottom,   but samples for closer examination were also taken at the same locations as the photographs.   The finest sand recovered from the shelf was taken from a point near the end of the sand spit, 5 km from the shore.   This was close to the most turbid water observed on each trip.   The sandy bottom 1km from the shore was protected by dense sea grass as shown in the photograph.   The coarsest sand was recovered from the edge of the shelf where the clearest water was consistently observed.

Further evidence of the influence of wind waves was provided by the first trip.   When the boat arrived at the buoy 5 km from the shore, a northerly wind of about 12 kn had been blowing for some 4 hours and had produced waves about 0.6 m high, with a period of about 2.5 s.   From the table reproduced by Phillips(ref.12),   showing the relation between wind and sea state,   the observations are consistent with waves of about 10 m wavelength.   Since the water was only 6 m deep at this point, it was shallow enough for waves of this length to produce a substantial movement of water across the bottom.   This produced the most turbid water encountered on the trip, having an attenuation coefficient of 1.9 m^{-1}.   When the boat returned to this position over four hours later, after the wind had dropped and the waves were only about 0.2 m high, the attenuation coefficient had fallen to 0.8 m^{-1}(as shown in figure 3). In other words, the most turbid water was observed when the waves were large enough to stir up sediment from the bottom.

In the deeper water a different pattern emerges.   Figures 3, 4 and 5 all show (or at least hint at) horizontal layers of water of different turbidity in the deep water away from the edge of the shelf.   The observations during November and December show a body of clear water below about 10 m deep.   Since the weather is warm at this time of year a stable thermocline may be assumed and the clear region may be identified as cool ocean water entering the gulf.

Further evidence for this identification was provided by the divers, who reported a strong northward current at the edge of the shelf. The photograph in figure 3 at the edge of the shelf shows sea grass being bent in one direction by this current. The more turbid surface water in November and December may be warmer more turbid water that has drifted from the coastal shelf.

The pattern is reversed for the observations in June, during winter. The deeper water was then more turbid and clearer water was found near the surface. This suggests that during winter the ocean water is less dense and enters the gulf on the surface, while the northern, more saline water drains out of the gulf along the bottom.

The influence of tides on water turbidity is not clear. The measurements in deep water were made during a spring low tide on the first trip, during a neap high tide on the second trip, and during an ebbing neap tide on the third trip. In the shallow water, the measurements were made during a flowing spring tide on the first trip and during neap low tides on the second and third trips. No relationship between the tide and the turbidity distribution is apparent, with one possible exception. The most turbid water was observed in shallow water on 23 November 1976, when (as mentioned above) the wind had generated large enough waves to disturb the bottom sediment. However, since the tide was flowing fast over the sand spit at the time, it could also have contributed to the turbidity by lifting sediment from the sand spit.

5. ATTENUATION OF LASER PULSE IN WATER

The attenuation of the laser pulse reflected from the sea bed can be described by a coefficient k, which is defined as the effective attenuation of the pulse per metre of water depth. The received radiant flux is then given by

$$F = F_o \exp \left[-2 \int_o^d k(z)dz \right] , \qquad (3)$$

where d is the water depth, the factor 2 accounts for both downward and upward transits of the pulse, and F_o is the received flux at zero depth.

In order to estimate the pulse attenuation coefficient from the data presented in figures 4 and 5, a theoretical model must be assumed. Therefore, the effective pulse attenuation coefficient is assumed to be a linear function of the beam attenuation coefficient c, namely

$$k = f + gc. \qquad (4)$$

The equation for the received flux then reduces to

$$Q = Q_o - fd - gD , \qquad (5)$$

where

$$Q = \tfrac{1}{2} \ln F ,$$

$$Q_o = \tfrac{1}{2} \ln F_o ,$$

and

$$D = \int_o^d c(z) \, dz$$

is a dimensionless quantity, which we call the "attenuation depth". Since both the depth and turbidity of the water vary between laser return signals, the data must be analysed statistically.

Equation (5) was used as the basis for multi-linear regression analysis of the data. The water depth was determined from the laser return signal. The attenuation depth was calculated by numerically integrating the beam attenuation coefficient. The logarithm of the bottom pulse amplitude was calculated after taking into account the gain of the photomultiplier at different applied voltages. The residual variation, due to such factors as transmitted peak laser power and bottom reflectivity, was assumed to be random. Regression analysis of the data obtained in Gulf St Vincent on 17 December 1976 and 10 June 1977 and in Cairns waters on 27 June 1977 yielded the following results:

$$Q_o = 1.9 \pm 0.1$$

$$f = 0.021 \pm 0.006 \ m^{-1}, \tag{6}$$

and

$$g = 0.13 \pm 0.03$$

One point from the Cairns data, which departed substantially from the trend of the other data, was omitted from the analysis. The suspect point, which was derived from oscillogram (a) in figure 8, could have been influenced by a change in turbidity during the time between the aircraft and boat measurements.

An appreciation of the suitability of the linear approximation assumed in equation (4) can be gained by plotting the mean pulse attenuation coefficient defined by

$$\bar{k} = (Q_o - Q)/d \tag{7}$$

against the mean beam attenuation coefficient defined by

$$\bar{c} = D/d . \tag{8}$$

This is done in figure 6, which shows both the points calculated from equations (7) and (8) and the regression line defined by the data in equation (6). It can be seen that the linear function is consistent with the data, within the observed variation.

6. MEASUREMENTS IN CAIRNS WATERS

On 27 June 1977, the transmissometer was taken on board HMAS Barricade, an RAN patrol boat. Water transmittance measurements were made at the 9 points on the line between False Cape and Arlington Reef near Cairns, shown in figure 7. The distribution of attenuation coefficient over this section of water is shown in figure 8. The cleanest sea water yet observed was located between the submerged Green Island Reef and Arlington Reef. This water comes from the Pacific Ocean by a current driven by the south-easterly trade winds. Close to shore the water was very turbid and appeared from the air as a brown streak all along the coast.

The main factors influencing water turbidity in North-Queensland waters are

different from those applicable in Gulf St Vincent. Of the factors at the beginning of Section 4, drainage from the land is of great significance, because North-Queensland has a high rainfall. The sediment which is carried to the sea by rivers, remains in suspension for a time determined by the size of the particles. When it finally settles on the bottom it adds to the fine mud that is common along the North-Queensland shore.

The turbid water close to the shore was observed to move northward, with the coastal current driven by the south-easterly trade winds. The near vertical contours of attenuation coefficient over much of the water indicate that strong vertical mixing was taking place. The 60 m wavelength swell observed in the area would have agitated the bottom sediment to some extent to a depth approaching 30 m. Wave action over the shallow coastal shelf could be a significant factor in keeping the sediment in suspension.

While the transmittance measurements were being made from the boat, the WRELADS system again was flown overhead in an aircraft. Some signal returns of the green channel are presented in figure 8. The sequence of traces (a) to (f) is arranged so that it resembles the profile of the bottom in the figure below. Trace (a) is one of a small number showing a bottom return about 5km from the shore. No bottom return apart from these was seen between the shore and the Green Island Reef, because the water was too turbid in this region. The sequence (b), (c), (d), (e), recorded up one side and down the other side of Green Island Reef, show a backscatter envelope that gradually decreases in magnitude as the water becomes clearer. In the clear water at the edge of Arlington Reef in traces (f) and (g) the backscatter is negligible. Traces (a), (b), (e) and (f) all represent extinction depths in water of different turbidities.

7. SPECTRAL DEPENDENCE OF WATER ATTENUATION COEFFICIENT

Water transmittance measurements at six different wavelengths were made 2 m below the surface at the nine points marked in figure 7 on the line between Arlington Reef and False Cape. The beam attenuation coefficients calculated from these data are presented in figure 9, with the locations numbered from Arlington Reef. The curves for locations 4 and 6 are omitted because they lie close to curves 5 and 7 respectively. The shaded area at long wavelengths shows the range of data for pure water, taken from figure 1.

The results are similar to those obtained by Clarke and James(ref.6), which are shown in figure 1. In both cases, the minimum attenuation coefficient varies from about 0.1 m^{-1} in clean ocean water to about 2 m in turbid coastal water. The wavelength, at which the minimum attenuation occurs, is just below 500 nm in clear water and moves to longer wavelengths as the water becomes more turbid.

It can be seen that the wavelength of the frequency doubled Nd:YAG laser, namely 532 nm, is a suitable choice for penetration of a wide range of water types.

Penetration of the water to greater depths is theoretically possible either by increasing the peak power of the laser pulse or by producing the same peak power at the optimum wavelength for each water type. It can be shown that the extinction depth (d_e) is increased by the same amount, either

by increasing the laser output power by a factor G or by choosing a wavelength at which the beam attenuation coefficient is reduced by Δc, if

$$G = \exp (2 d_e g \Delta c) . \tag{9}$$

This expression assumes that the spectral dependence of the system attenuation coefficient k is identical to that of the beam attenuation coefficient c. With this assumption together with the measured extinction depths (discussed

in the next section) and the data in figure 9, it follows that an increase in laser output power of 10% in turbid water and 20% in clear water would be enough to match any improvement obtained by optimizing the wavelength.

8.   DEPENDENCE OF EXTINCTION DEPTH ON WATER TURBIDITY

One of the most useful parameters for describing performance of the laser airborne depth sounder is the extinction depth, that is, the maximum depth at which the ratio of the bottom signal to limiting noise is unity.   The meaning of the term may be gauged from the signal returns considered in this report to exemplify measurements of extinction depths.   As mentioned in previous sections, examples are oscillogram (i) in figure 5 and oscillograms (a), (b), (e) and (f) in figure 8.

When parameters applicable to an extinction case are designated by a subscript e, equation (5) becomes

$$Q_e = Q_o - fd_e - dD_e. \tag{10}$$

Using for Q_e, f and g the values given in equation (6) together with the observed values of d_e and D_e for the four most reliable of the five cases listed above (excluding (a) in figure 8), yields four values of Q_e. Their mean and standard deviation are given by

$$Q_e = 0.5 \pm 0.1 . \tag{11}$$

A theoretical expression for the dependence of extinction depth on beam attenuation coefficient, which depends only on the assumptions made in Section 5 of this report, can be derived from equations (8) and (10).

$$d_e = (Q_o - Q_e)/(f + g\bar{c}) \tag{12}$$

and a similar expression can be derived for D_e.   Curves based on these expressions and the value of Q_e given in equation (11) are shown in figure 10, together with the observed extinction depths and extinction attenuation depths.   The use of Q_e from equation (11) ensures that the theoretical curves and the experimental points have the same average magnitude.   The tendency of the experimental points to follow the dependence of the theoretical curves on the mean beam attenuation coefficient confirms the usefulness of the theoretical model.   The points corresponding to oscillogram (a) in figure 8, which are at the right of figure 10, appear to overestimate either the depths or the beam attenuation coefficient.

The dynamic range of the receiver must exceed the ratio of the received flux at zero depth to that at the extinction depth, namely

$$F_o/F_e = \exp\left[2(Q_o - Q_e) \right]. \tag{13}$$

From the values of Q_o and Q_e given above, the minimum dynamic range of the receiver with its annular field of view is about 15:1. Since, in relatively clear water, the dynamic range increases when the background light level falls (e.g. under heavy cloud or at night) a dynamic range larger than 15:1 will be needed in practice.

9.   CONCLUSION

Measurements of the beam attenuation coefficient in both South Australian and Queensland coastal waters resulted in values ranging from 0.1 to 2 m^{-1}. This is comparable with the range reported by others. Over the spectral range 400 to 600 nm only a small dependence on wavelength was observed for each water type.   The minimum attenuation coefficient for a given water type was observed at a wavelength that ranged from less than 500 nm in clear water to more than 550 nm in turbid water.   This change in wavelength for minimum attenuation is also consistent with other published data.

The wavelength of the frequency doubled Nd:YAG laser, namely 532 nm, was confirmed as suitable for penetration of a wide range of water types.   If the system attenuation coefficient has the same spectral dependence as the beam attenuation coefficient, the improved depth-measuring performance expected from a variable wavelength laser of the same power could be achieved with a 20% increase in the output power of the Nd:YAG laser.   The increased complexity of a variable wavelength system would therefore be unjustified.

The effective attenuation coefficient (k) of the laser pulse recorded by the depth sounding systems was found to be very much smaller than the measured beam attenuation coefficient (c) of the water.   The reason is that the depth sounder collects a large fraction of the scattered light, which is excluded in the measurement of the beam attenuation coefficient.   Regression analysis of the data yielded the following empirical relationship:

$$k = 0.021 + 0.13 c .$$

The extinction depth, that is the maximum measurable depth in a given type of water, was found to be inversely proportional to the system attenuation coefficient k. When the peak power of the transmitted laser pulse was about 1 MW, the extinction depth was given by

$$d_e = 1.4/k .$$

Because this is dependent on k rather than c, it corresponds to the range from below 4 to above 10 beam attenuation lengths.

The results suggest three important influences on the turbidity of shallow coastal water.   Firstly, the quantity of sediment suspended in the water and lying on the bottom is governed by the amount of rainfall on adjacent coastal land.   Secondly, the amount of sediment suspended in the water is determined by the nature of the bottom, the water depth, and the size of waves agitating the bottom.   Thirdly, bulk water movement due to tides and currents carry both turbid and clear water to new locations.   Further studies are needed to establish the relative importance of these processes.

10.   ACKNOWLEDGEMENTS

REFERENCES

No.	Title	Title
1	Clegg, J.E. and Penny, M.F.	"Depth Sounding from the Air by Laser Beam". Journal of Navigation, Vol.31, pp 52-61, 1978
2	Abbot, R.H. and Penny, M.F.	"Air Trials of an Experimental Laser Bathymeter". WRE-TN-1509(AP), 1975
3	Abbot, R.H., Watts, G.J. and Penny, M.F.	"Wrelads I Trials Report". ERL-0026-TR, 1978
4	Smith, R.C. and Tyler, J.E.	"Transmission of Solar Radiation into Natural Waters". Photochem. Photobiol. Rev., Vol.1, pp 117-155, 1976
5	Tyler, J.E. (Ed.)	"Light in the Sea". Benchmark Papers in Optics, Vol.3 Dowden, Hutchinson, & Ross, Pennsylvania, 1977
6	Clarke, G.L. and James, H.R.	"Laboratory Analysis of the Selective Absorption of Light by Sea Water" J. Opt. Sec. Amer., Vol.29 pp 29-55, 1939
7	Koerber, B.W.	"Light Propagation in Water" WRE-TN-1694(AP), 1976
8	Watts, G.J.	"A Preliminary Analysis of Secchi Disc Measurements taken in Australian Waters" OSD Memorandum 75/4, 1975
9	Woodcock, B.	"An Underwater Transmissometer" WRE-TN-1461(AP), 1975
10	Austin, R.W. and Petzold, T.J.	"Considerations in the Design and Evaluation of Oceanographic Transmissometers". In Tyler (ref.5), pp 104-120, 1977
11	Williams, J.	"Optical Properties of the Sea" US Naval Institute, Annapolis, 1970
12	Phillips, D.M.	"Wind, Sea and Swell around the Australian Coast" WRE-TN-1628(AP), 1976
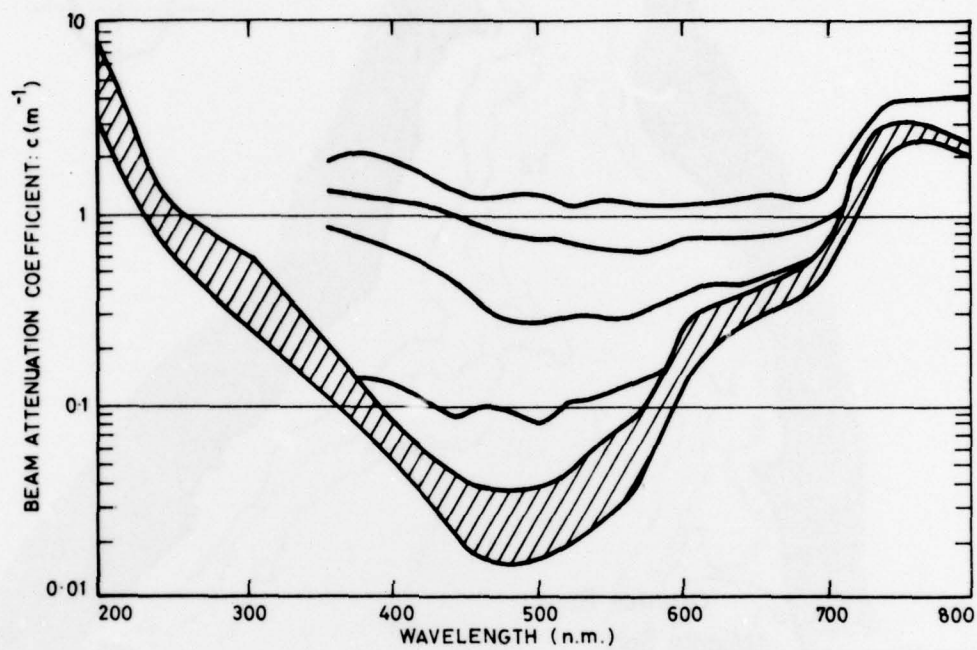
Figure 1.   The beam attenuation coefficient of different
types of water as a function of wavelength
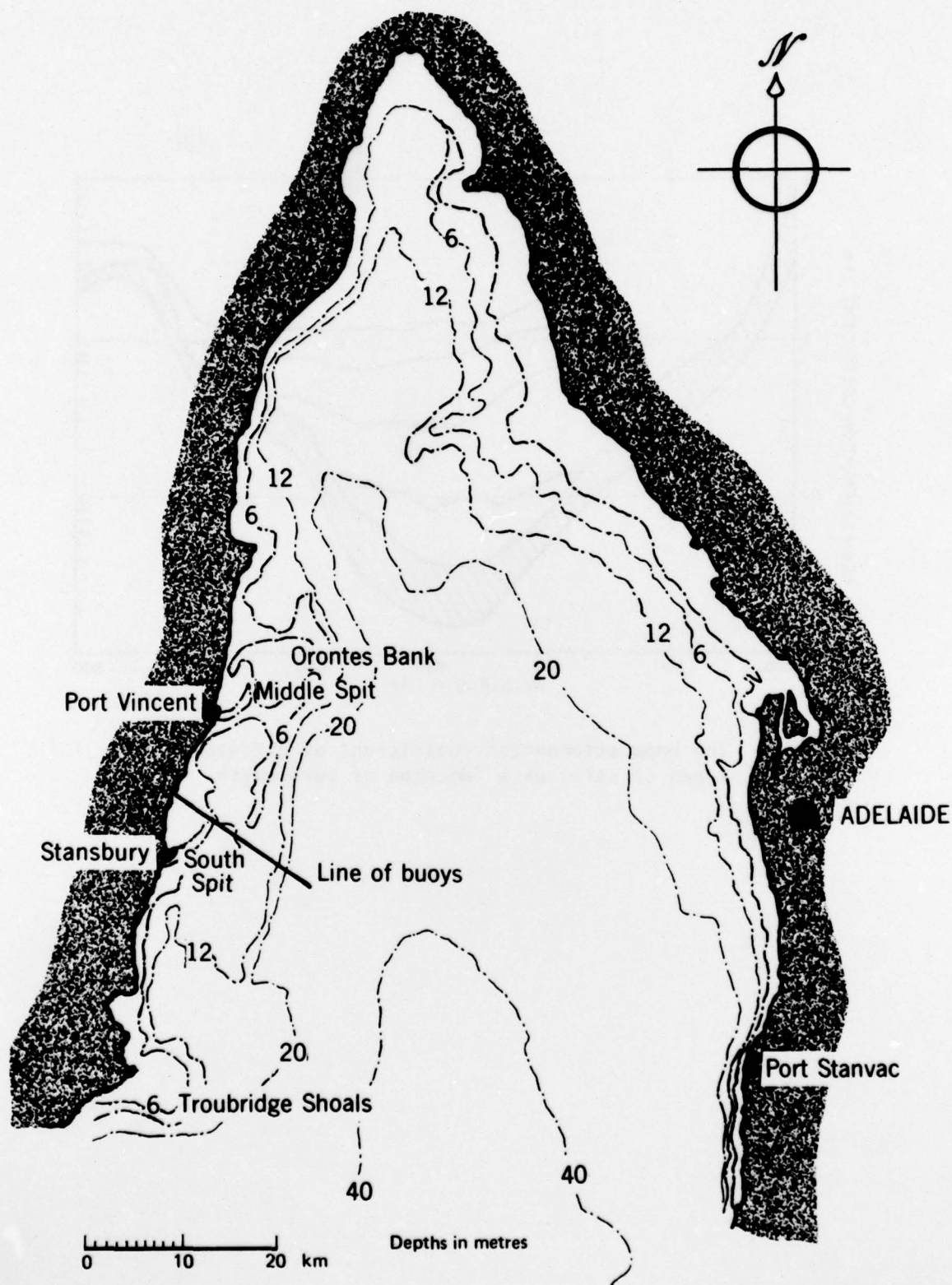
Figure 2. Chart of Gulf St. Vincent showing the line of
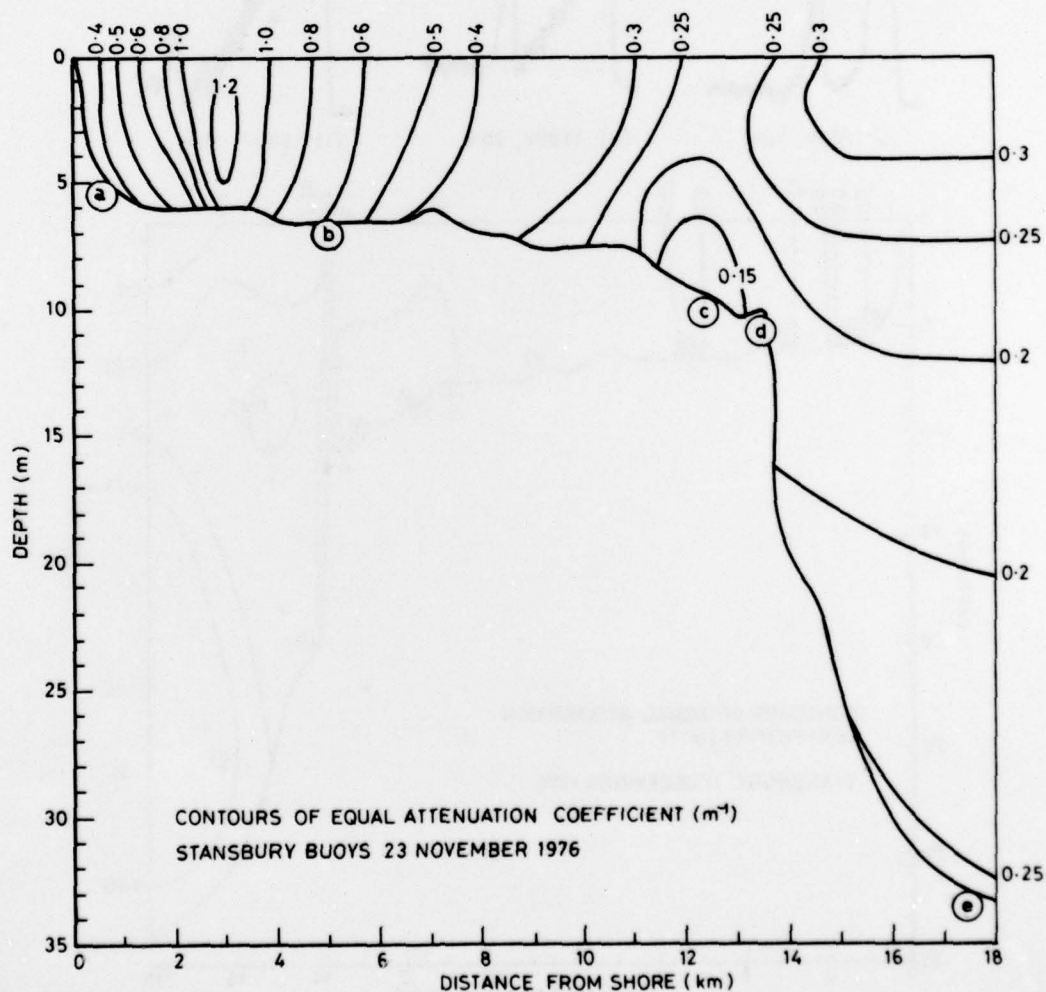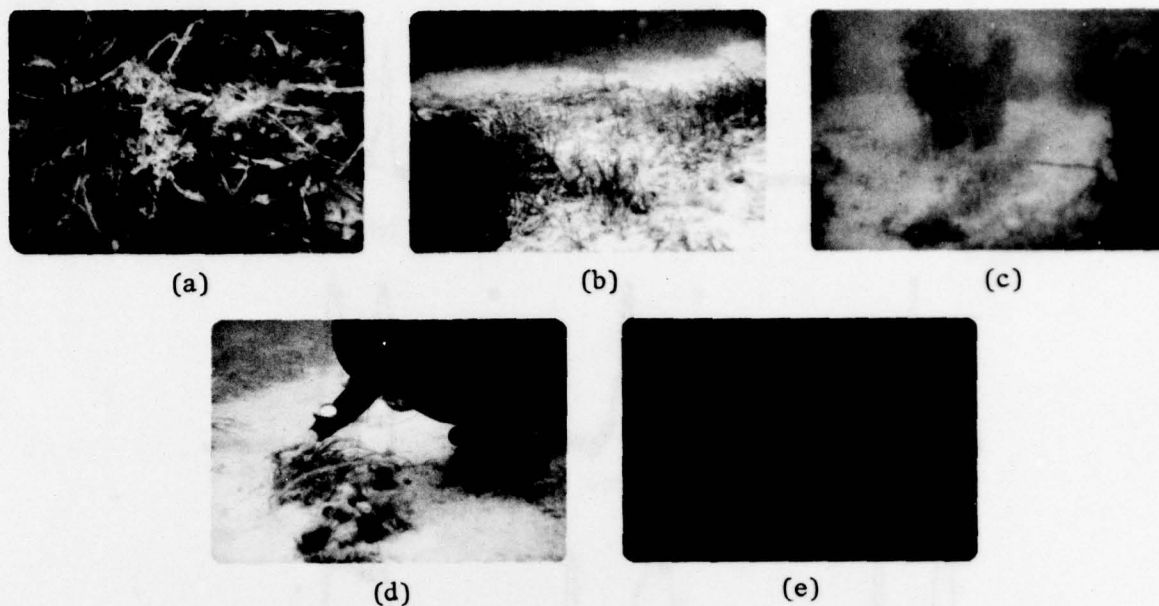buoys near Stansbury

Figure 3. Measured distribution of beam attenuation coefficient of
the water and photographs of the bottom along the
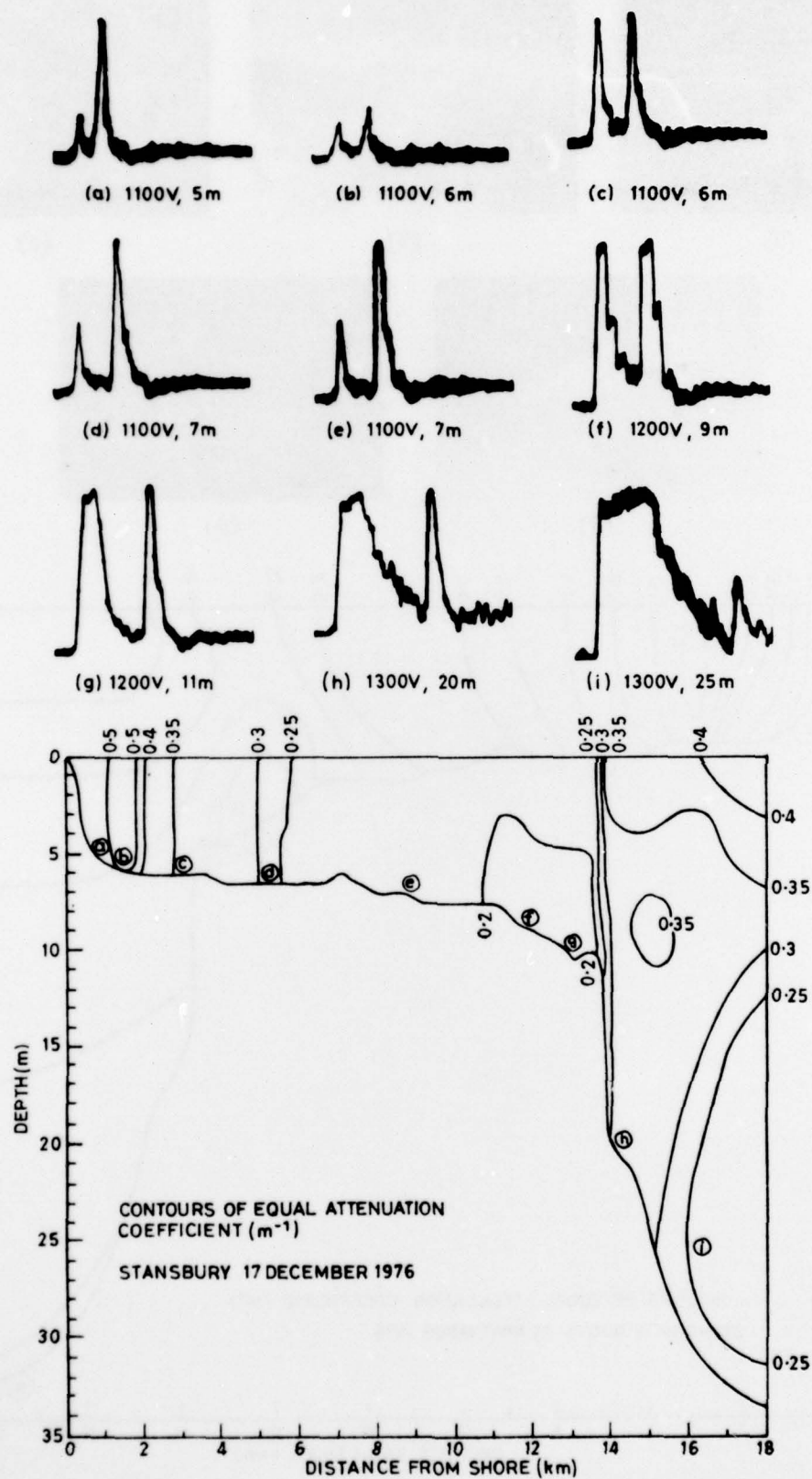Stansbury line of buoys on 23 November 1976

Figure 4.   Measured distribution of beam attenuation coefficient of
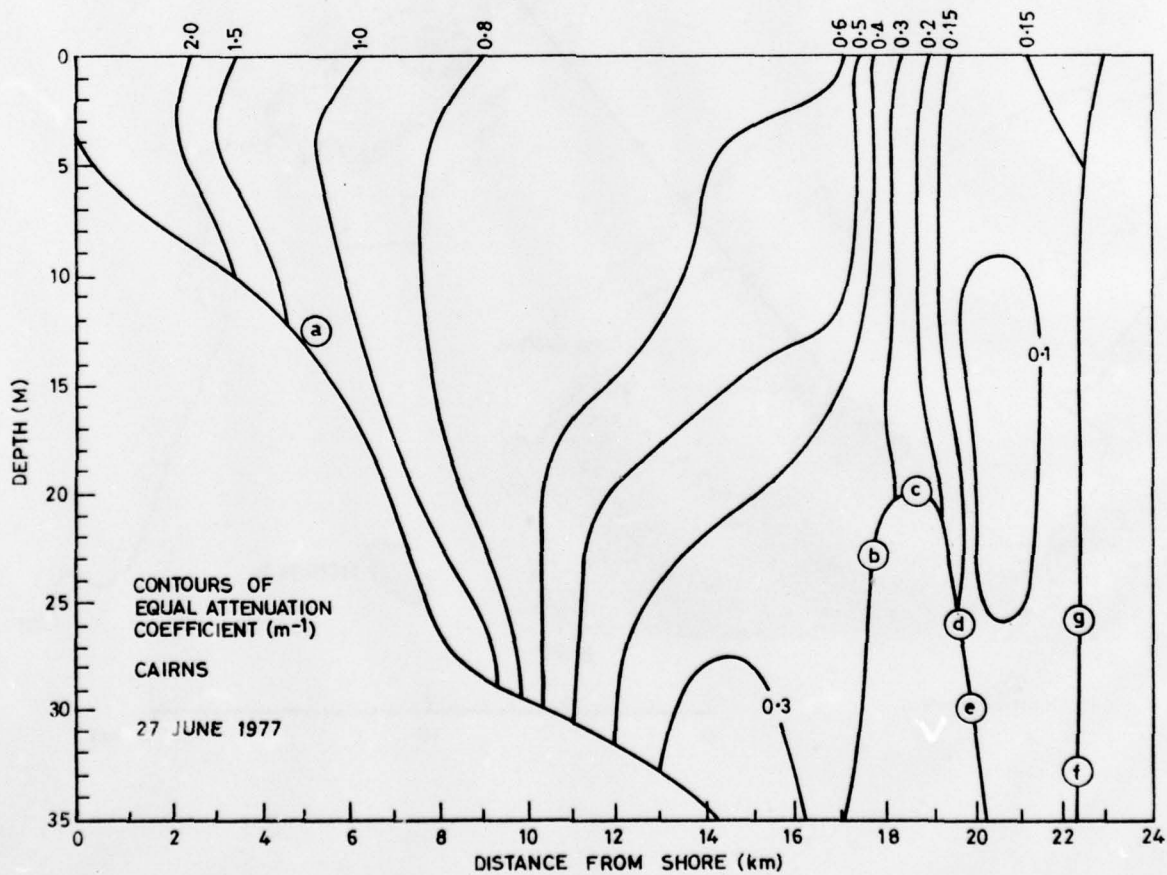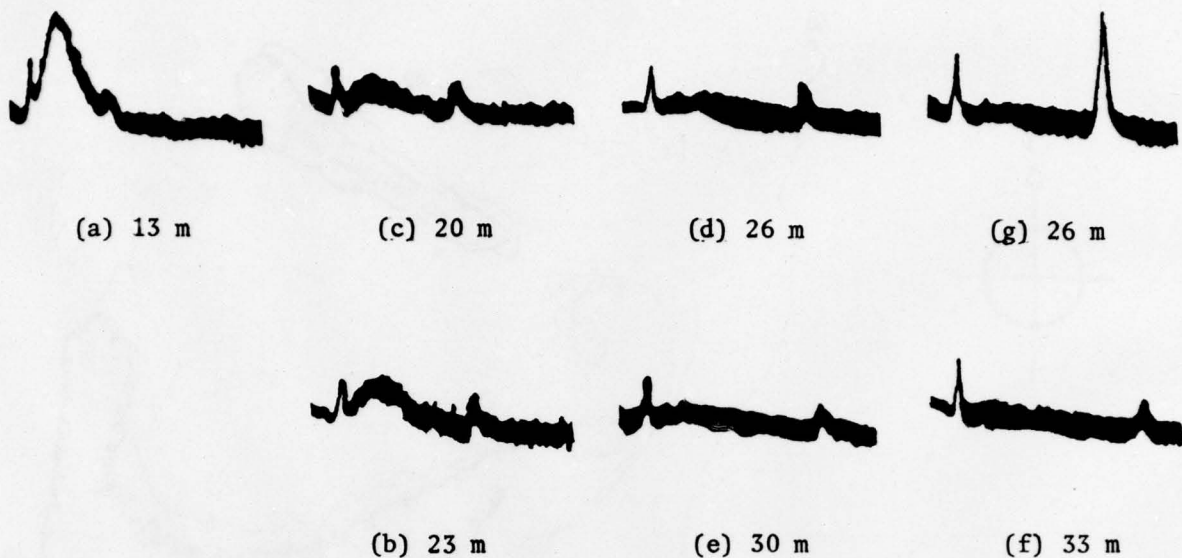the water and airborne laser return signals along the
Stansbury line of buoys on 17 December 1976
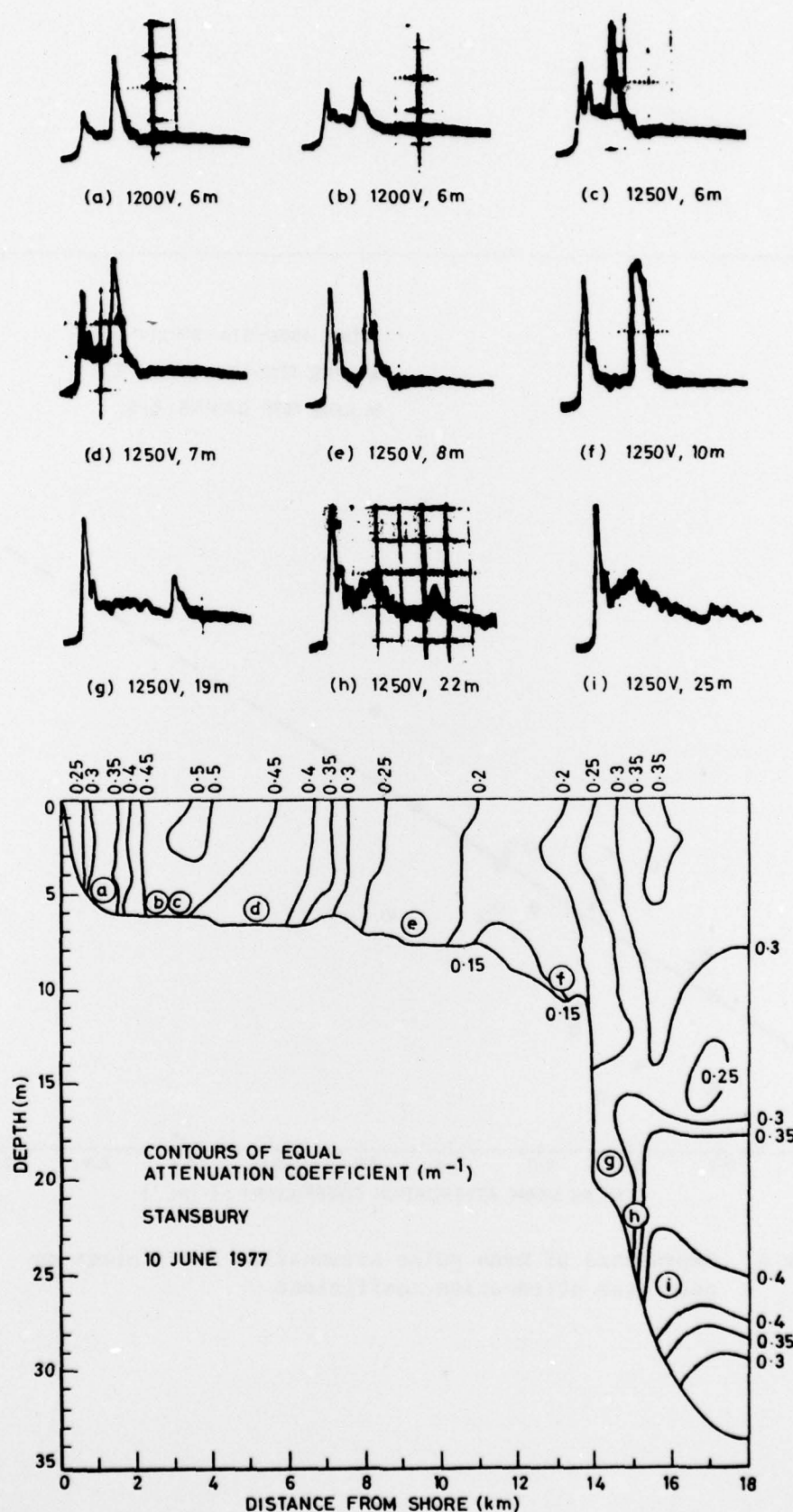
Figure 5. Measured distribution of beam attenuation coefficient
of the water and airborne laser return signals along
the Stansbury line of buoys on 10 June 1977

ERL-0072-TR
Figure 6
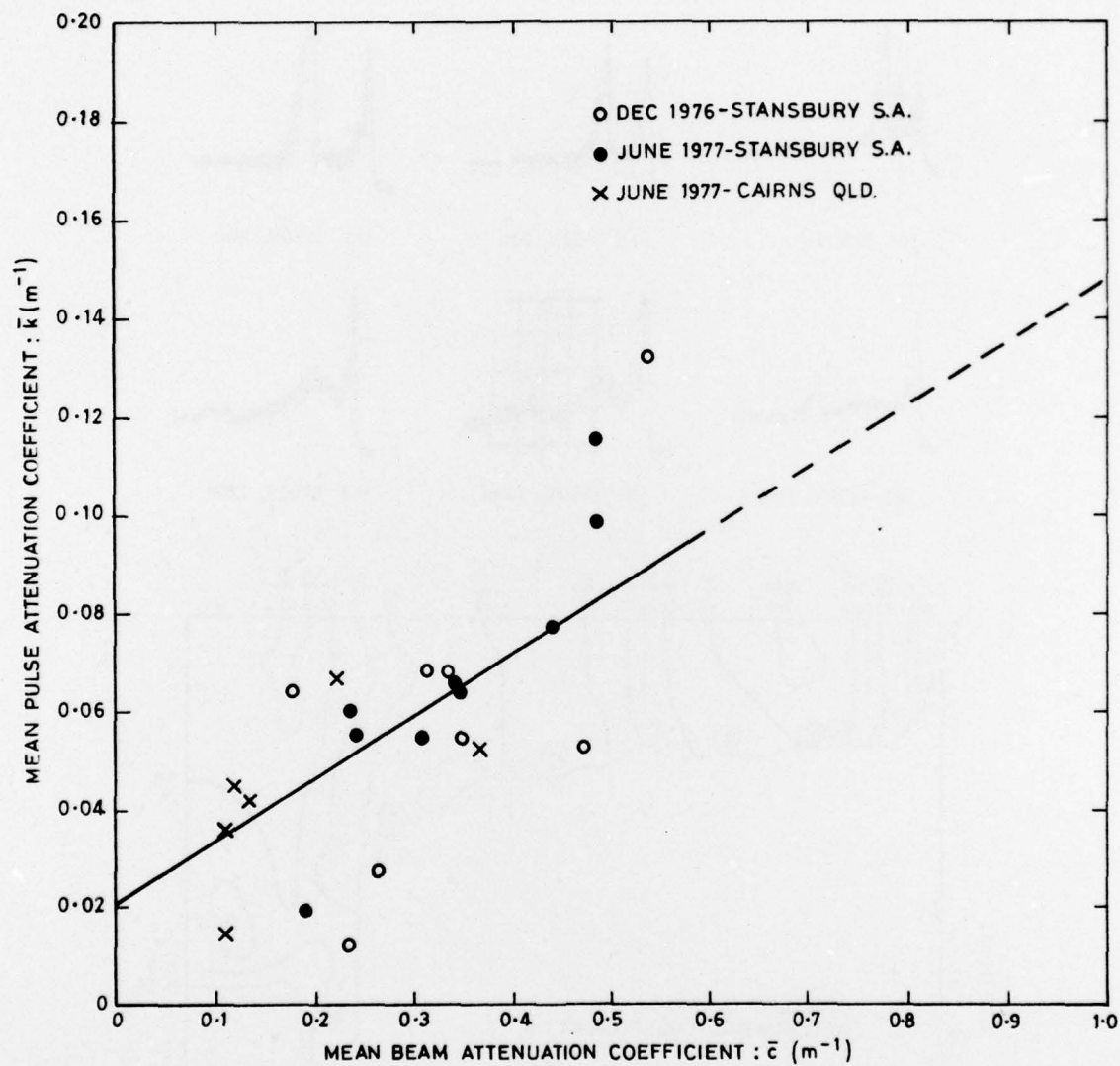
Figure 6.   Dependence of mean pulse attenuation coefficient on
mean beam attenuation coefficient
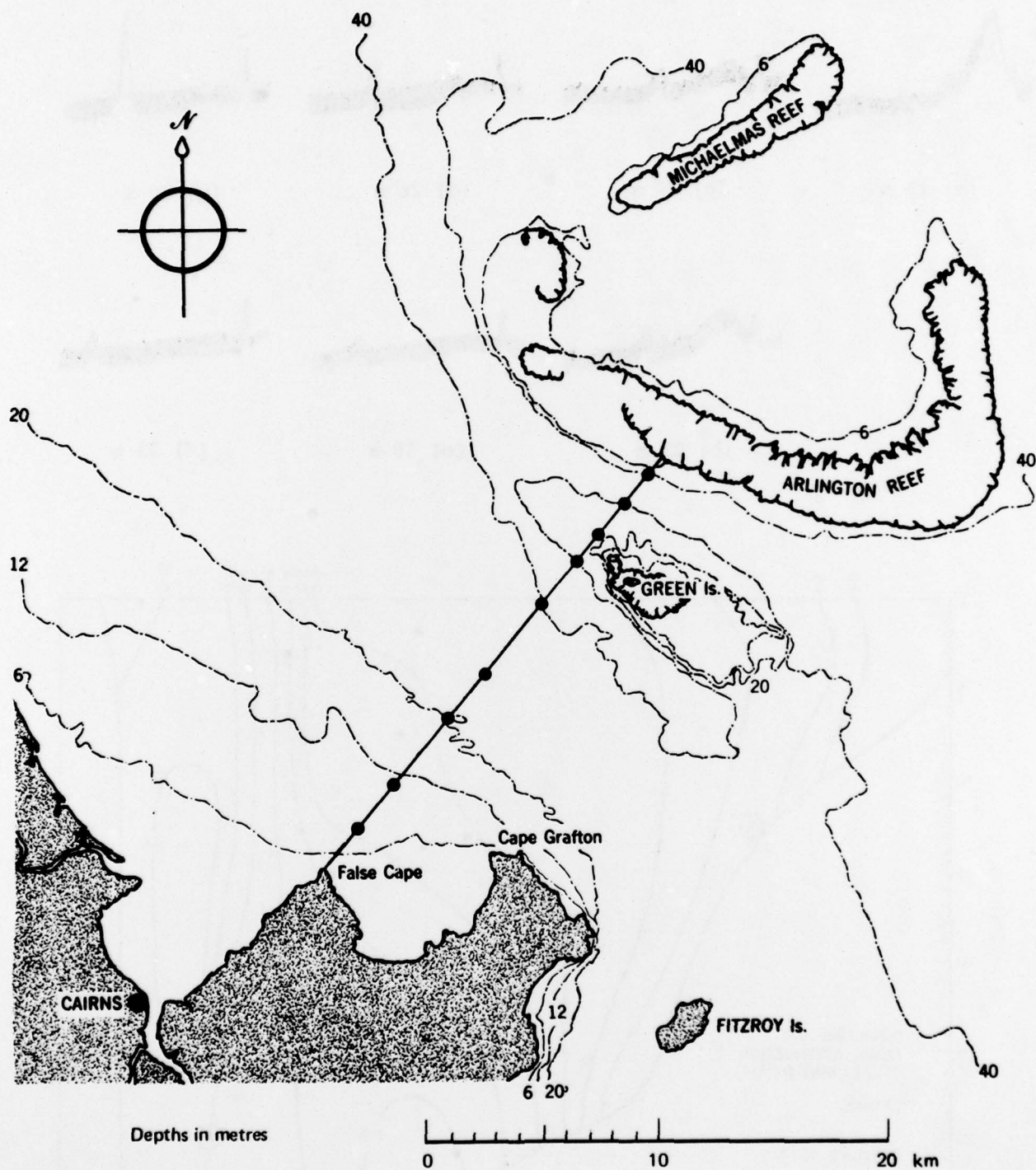
Figure 7. Chart of Cairns waters showing locations of transmittance
measurements

Figure 8.   Measured distribution of beam attenuation coefficient of
the water and airborne laser return signals near Cairns
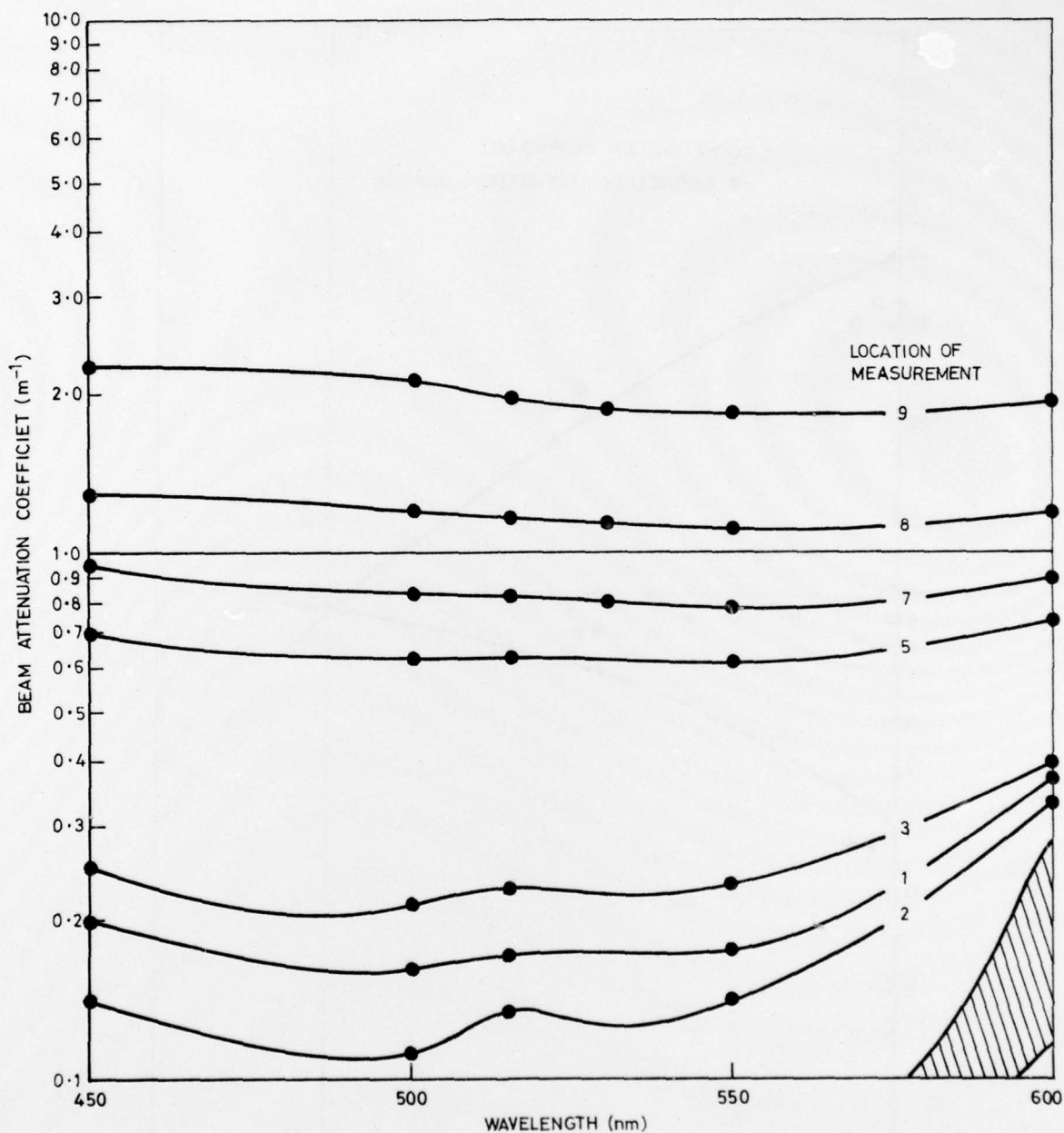on 27 June 1977

Figure 9.   The beam attenuation coefficient of different types
of water near Cairns as a function of wavelength
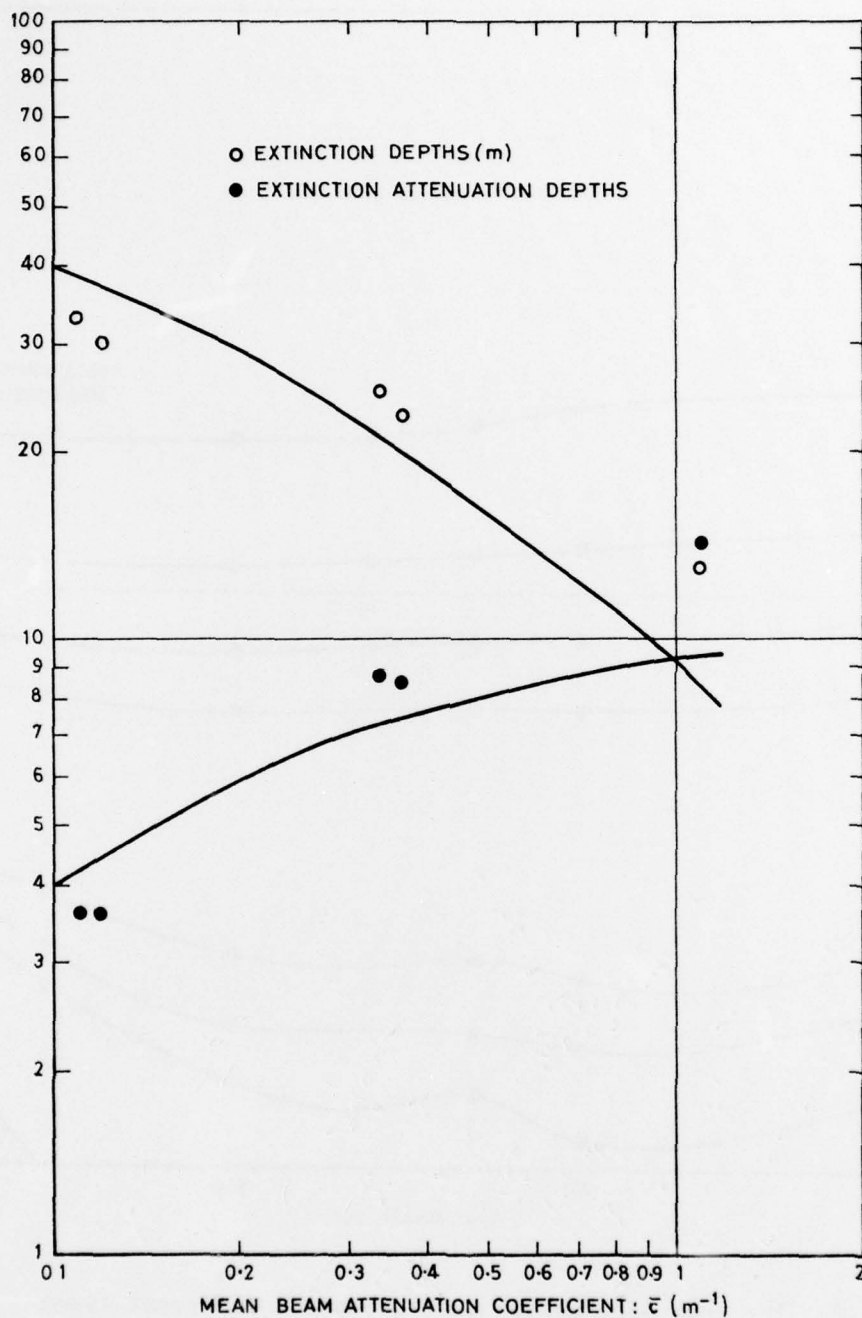
ERL-0072-TR
Figure 10

Figure 10. Dependence of extinction depth and extinction attenuation
depth on mean beam attenuation coefficient

DISTRIBUTION

Copy No.

EXTERNAL

In United Kingdom

Defence Scientific and Technical Representative, London	1
Research and Development Representative, London	2

In United States of America

Counsellor, Defence Science, Washington	3
Defence Research and Development Attache, Washington	4 - 5

In Australia

Chief Defence Scientist	6
RAN Hydrographer	7 - 8
Deputy Chief Defence Scientist	9
Controller, Programmes and Analytical Studies	10
Superintendent, Science and Technology Programmes	11
Navy Scientific Adviser	12
Superintendent, Analytical Studies	13
Officer-in-Charge, RAN Trials and Assessing Unit	14
Director of Naval Meteorology and Oceanographic Services	15
Director, Division of National Mapping, Department of National Resources	16
Director, Joint Intelligence Organisation (DDSTI)	17
Defence Information Services Branch (for microfilming)	18

Defence Information Services Branch for:

United Kingdom, Ministry of Defence Defence Research Information Centre (DRIC)	19
United States, Department of Defense, Defense Documentation Center	20 - 31
Canada, Department of National Defence, Defence Science Information Service	32
New Zealand, Ministry of Defence	33
Australian National Library	34